Precipitation diagram of calcium carbonate polymorphs: its construction and significance

2009 J. Phys.: Condens. Matter 21 425102

(http://iopscience.iop.org/0953-8984/21/42/425102)

J. Phys.: Condens. Matter **21** (2009) 425102 (6pp) doi:10.1088/0953-8984/21/42/425102

Precipitation diagram of calcium carbonate polymorphs: its construction and significance

Jun Kawano[1,2], **Norimasa Shimobayashi**[1], **Akira Miyake**[1] and **Masao Kitamura**[1]

[1] Department of Earth and Planetary Science, Faculty of Science, Kyoto University, Kitashirakawa-Oiwake, Sakyo-ku, Kyoto 606-8502, Japan
[2] GAAJ-ZENHOKYO Laboratory, Gemmological Association of All Japan, 8F Daiwa-Ueno Building 5-25-11 Ueno Taito-ku, Tokyo 110-0005, Japan

E-mail: miya@kueps.kyoto-u.ac.jp

Received 25 May 2009, in final form 12 August 2009
Published 8 September 2009
Online at stacks.iop.org/JPhysCM/21/425102

Abstract
In order to interpret the formation mechanism of calcium carbonate polymorphs, we propose and construct a new 'precipitation diagram', which has two variables: the driving force for nucleation and temperature. The precipitation experiments were carried out by mixing calcium chloride and sodium carbonate aqueous solutions. As a result, a calcite–vaterite co-precipitation zone, a vaterite precipitation zone, a vaterite–aragonite co-precipitation zone and an aragonite precipitation zone can be defined. Theoretical considerations suggest that the steady state nucleation theory can explain well the appearance of these four zones, and the first-order importance of the temperature dependency of surface free energy in the nucleation of aragonite. Furthermore, the addition of an impurity will likely result in the change of these energies, and this precipitation diagram gives a new basis for interpreting the nature of the polymorphs precipitated in both inorganic and biological environments.

1. Introduction

Calcium carbonate, $CaCO_3$, has several different schemes of atomic arrangements or polymorphs. At room temperature and pressure only calcite is stable thermodynamically and expected to form predominantly. However, exceptions are widely known such as the shells of shellfish consisting dominantly of aragonite, or many organisms forming their tissues with various polymorphs of calcium carbonate (Weiner and Dove 2003). Therefore, the ability to select and use these polymorphs for their own functional requirements is fundamental to the life cycle of these animals, and the formation conditions of different polymorphs are important. In order to understand this kind of bio-genetic formation, it is necessary to understand the physical principle of inorganic formation of calcium carbonate polymorphs from solution, which can reveal what makes the formation of calcium carbonate polymorphs in a biological process unique. For more than a century, precipitation of calcium carbonate polymorphs from a variety of solutions has attracted research (Johnston *et al* 1916, Kitano 1962a, 1962b, Shönel and Mullin 1982, Ogino *et al* 1987, Clarkson *et al* 1992, Falini *et al* 1994). As a result, a great number of controlling phenomena, such as impurity effect (Kitano 1962a, 1962b, Shönel and Mullin 1982, Falini *et al* 1994), have been proposed to account for the formation of a particular polymorph, however their physical basis is poorly understood.

Here, we construct a new precipitation diagram showing which phase first precipitates from a solution under a given condition. Two variables: the driving force for nucleation and temperature are adopted in the diagram, and the well-studied $CaCl_2$–Na_2CO_3 system (Shönel and Mullin 1982, Ogino *et al* 1987, Clarkson *et al* 1992) was chosen for constructing the diagram. In addition, we choose an impurity-free system, except for sodium chloride, to keep the ionic strength constant, because the impurity effect has yet to be theoretically evaluated. On the basis of this scheme, precipitation experiments were carried out, and the conditions were defined under which three polymorphs of $CaCO_3$ (calcite, aragonite and vaterite) form.

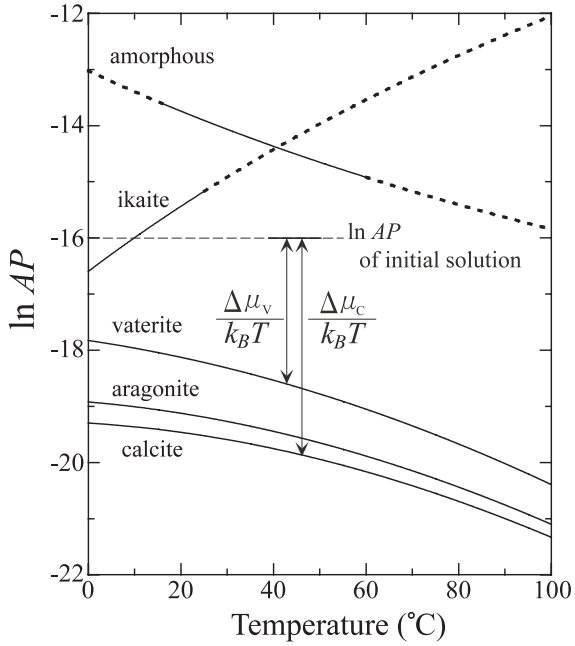

Figure 1. Construction of a precipitation diagram, where the horizontal axis is the natural logarithm of the activity product of calcium and carbonate ions, ln AP, and the vertical axis is the temperature. Equilibrium curves for the formation reaction of polymorphs of calcium carbonate (calcite, aragonite, vaterite, and ikaite) and amorphous calcium carbonate, which are calculated from their equilibrium constants (Clarkson *et al* 1992, Plummer and Busenberg 1982, Biscoff *et al* 1993) are shown. The equilibrium curve for calcite is the lowest, indicating that calcite is a stable phase throughout the whole temperature range of the diagram. The driving force for nucleation of phase i ($\Delta\mu_i/k_BT$) is equal to the difference between ln AP of the initial solution and its corresponding equilibrium curve at a given temperature. As examples, the driving force for nucleation of calcite $\Delta\mu_C/k_BT$ and vaterite $\Delta\mu_V/k_BT$ in the same initial solution is illustrated in the figure.

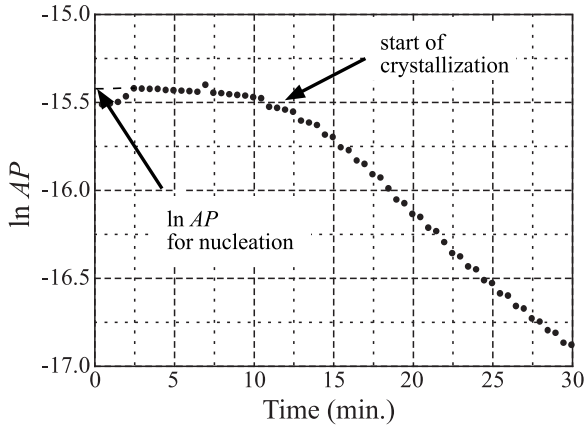

Figure 2. Change in ln AP of the mixed solution with time when 3.0×10^{-3} mol l^{-1} solutions were mixed at 20 °C. In this case, ln AP shortly after mixing is almost constant at −15.43, and this value is taken as ln AP for nucleation in the run.

2. Basic concept

The driving force for nucleation of one of the polymorphs (phase i) from an aqueous solution by the reaction of $Ca^{2+} + CO_3^{2-} \rightarrow CaCO_3$ (i) is expressed as $\Delta\mu_i/k_BT$, where $\Delta\mu_i$ is the difference of chemical potentials for the reaction, k_B the Boltzmann constant, and T the absolute temperature. The equilibrium constant for phase i, K_i, is expressed as $K_i \equiv a^0_{Ca^{2+}} \cdot a^0_{CO_3^{2-}}$, where a_0 denotes the activity at the saturated state. Similarly, the activity product of calcium and carbonate ions, AP, is defined as $AP \equiv a_{Ca^{2+}} \cdot a_{CO_3^{2-}}$ where a denotes the activity (De Yoreo and Vekilov 2003). The driving force for nucleation of phase i is given as:

$$\Delta\mu_i/k_BT = \ln AP - \ln K_i. \quad (1)$$

Thus, the precipitation diagram can be expressed by plotting ln AP against T. The equilibrium constants for calcite, aragonite, vaterite, ikaite, and amorphous calcium carbonate (ACC) have been published (Clarkson *et al* 1992, Plummer and Busenberg 1982, Biscoff *et al* 1993) and are illustrated in the ln AP–T diagram (figure 1). The relative positions of the equilibrium curves in figure 1 are related to the relative stabilities of the polymorphs; that is, throughout the whole temperature range of the diagram, calcite is stable, both aragonite and vaterite are metastable, and aragonite is more stable than vaterite. $\Delta\mu_i/k_BT$ in equation (1) is expressed by the distance between ln AP of a solution and the equilibrium curve for phase i at a given temperature in the diagram, therefore each phase can nucleate only at the condition where ln AP is above its equilibrium curve. In this study, in order to understand the physical meanings of the nucleation phenomena for three crystalline phases, most of the experiments were conducted under the equilibrium curve of ACC where ACC can not form, although ACC has lately attracted attention (Addadi *et al* 2003).

3. Experimental details

Calcium carbonate was precipitated by pouring 200 ml of $CaCl_2$ and Na_2CO_3 solutions into a 500 ml water-jacketed beaker at the same time. Both solutions had been adjusted beforehand to the same concentration (5.0, 3.0, 2.0, 1.5, and 1.0×10^{-3} mol l^{-1}), that is, the Ca/CO_3 ratio is kept the same through all the present experiments. These solutions had been preheated to temperatures of around 20, 50, and 80 °C. The ionic strength of the mixed solution was kept at almost 0.1 during stirring with sodium chloride. The mixed solution was continuously stirred in the beaker sealed with a paraffin film, using a magnetic stirrer on a hot plate, which kept the solution at the desired temperature.

The activity product is related to both the pH and the calcium ion concentration (Morse and Mackenzie 1990). The pH and the calcium ion concentration were monitored every 30 s during the stirring, and were used for estimation of ln AP on the assumption that the partial pressure of CO_2 is constant. ln AP just after the mixing was almost constant for a certain period (figure 2), which indicates that the assumption for the partial pressure of CO_2 is appropriate, and is taken as ln AP for nucleation in the run. As precipitation started, ln AP decreased rapidly in all runs at 20 and 50 °C. In the runs at 80 °C, only

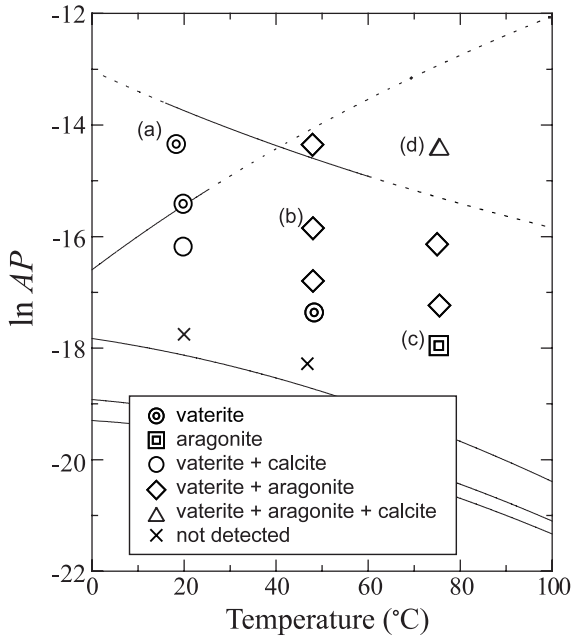

Figure 3. Precipitated polymorphs of calcium carbonate plotted in the precipitation diagram in figure 1. Double circles: precipitation of small spherules of vaterite, circle: co-precipitation of vaterite and calcite, double squares: precipitation of columnar aragonite, diamonds: co-precipitation of aragonite (short columns) and vaterite (hexagonal plates and spherules), triangle: co-precipitation of dendritic vaterite, columnar aragonite and calcite detected only by x-ray diffractometry, crosses: not detected because of too small an amount of precipitate. Photomicrographs of precipitates under the conditions marked (a)–(d) are shown in figure 4.

the pH was measured because a calcium ion selective electrode is available only below 50 °C. In this case, the activity of the calcium ion of the initial solution was calculated from the concentration of the initial solution. Also, since the pH value started to change with time just after stirring in this temperature condition, its initial value was also estimated by extrapolating from the change of pH with time. The induction period for nucleation of each polymorph was not measured in the present experiments, because co-precipitations of two or three polymorphs occur in several runs as described below.

After decreasing $\ln AP$ or the pH, the precipitates were recovered by a glass filter and dried in an oven at 110 °C. The recovered samples were observed under an optical microscope and examined by using an x-ray diffractometer.

4. Results

Polymorphs appearing in all runs (13 conditions) are plotted in the precipitation diagram (figure 3). Five distinct zones can be defined by the appearance of the polymorphs.

Calcite–vaterite co-precipitation zone. At 20 °C and $\ln AP = -16.20$, small (<10 μm in diameter) spherules of vaterite were observed. In addition, the formation of a little calcite was confirmed only by the x-ray powder diffraction.

Vaterite precipitation zone. In the runs where $\ln AP$ was above −16 at 20 °C and the run where the driving force for nucleation was the smallest at 50 °C, only small (<10 μm in diameter) spherules of vaterite were observed (figure 4(a)).

Vaterite–aragonite co-precipitation zone. In the relatively high $\ln AP$ conditions at 50 and 80 °C, both vaterite (hexagonal plates and spherules about 5–20 μm) and aragonite (short columns 5–20 μm in length) formed (figure 4(b)).

Aragonite precipitation zone. In the run where $\ln AP = -17.96$ at 80 °C, only columnar crystals of aragonite (5–20 μm in length) were observed (figure 4(c)).

Highly dis-equilibrium zone. In addition to the four zones described above, another zone can be defined where the $\ln AP$ value is higher than the equilibrium curve for ACC (figure 3). Previous experimental studies (Nancollas *et al* 1983, Ogino *et al* 1987, Clarkson *et al* 1992, Kawano *et al* 2002) indicate that the precipitates observed in the present study (figure 4(d)) may be formed after ACC. Therefore, data in this zone are omitted in further discussions, though ACC has lately attracted attention (Addadi *et al* 2003).

5. Discussion

In the present experiments, three polymorphs, calcite, aragonite and vaterite, were observed as precipitates. Here, the nucleation rates of three polymorphs based on the classical homogeneous nucleation theory are compared with each other, since the precipitation phenomena of crystals from aqueous solutions have been explained by that theory (e.g., Pina and Putnis 2002).

In nucleation theory (e.g., Toschev 1973, Markov 1995, Aaronson and Lee 1999), the steady state nucleation rate (J_0) is expressed as $J_0 = \omega^* \Gamma Z_1 \exp(-\Delta G^*/k_B T)$, where ω^* is the frequency of the attachment of molecules to the critical nucleus, Γ the Zeldovich factor, Z_1 the steady state concentration of single molecules, and ΔG^* the work of formation of the critical nucleus. In the case of solution growth, J_0 can be expressed as (Markov 1995);

$$J_0 = 2\nu\lambda\Omega(\gamma/k_B T)^{1/2} C^2 \exp(-\Delta U/k_B T) \times \exp(-\Delta G^*/k_B T), \qquad \Delta G^* = \frac{16\pi}{3}\frac{\gamma^3\Omega^2}{\Delta\mu^2}, \tag{2}$$

where ν is the frequency factor, λ the mean free path in the solution, Ω the molar volume of the molecules, which is calculated as the unit cell volume divided by the number of $CaCO_3$ in the cell in the present study, γ the surface free energy of the nucleus, C the number of molecules per unit volume in the solution, ΔU the activation energy for the attachment of molecules to the critical nucleus, and $\Delta\mu$ the chemical potential difference expressed in equation (1).

The non-steady state nucleation rate is expressed by J_0 and the induction period, τ, (Kashchiev 1969) and τ for solution growth is given as (Markov 1995);

$$\tau = \frac{16}{\pi}\frac{k_B T\gamma \exp(\Delta U/k_B T)}{(\Delta\mu)^2 C\nu\lambda}. \tag{3}$$

The present experimental result shows that the appearance of metastable phases is essential in the precipitation diagram

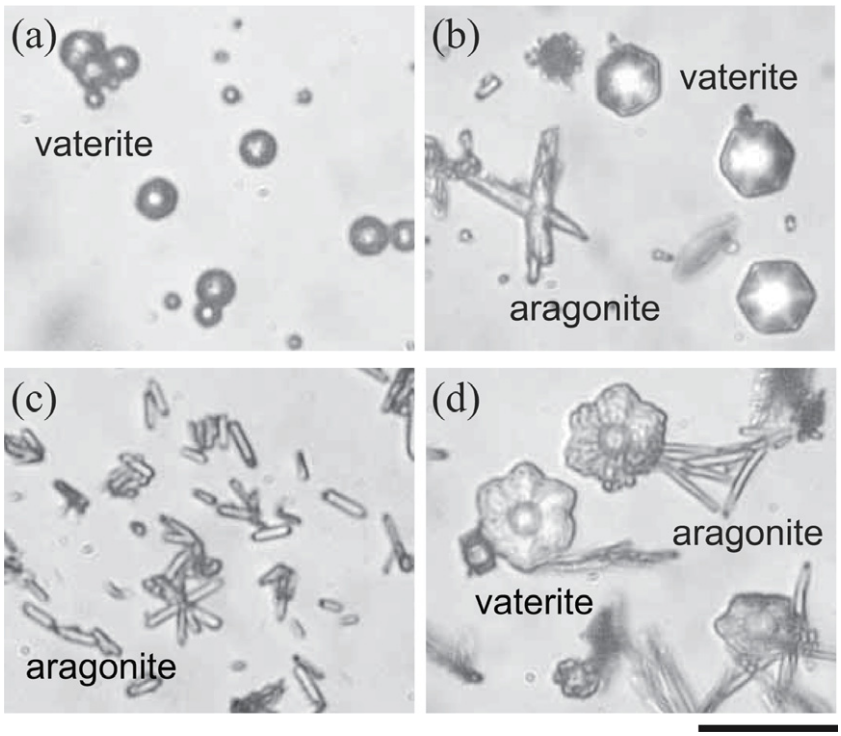

Figure 4. Photomicrograph of precipitates. (a)–(d) correspond to the conditions shown in figure 3. The magnifications of the micrographs are the same. The scale bar is 20 μm. (a) Small spherules of vaterite precipitated (5.0×10^{-3} mol l^{-1} solutions at 20.0 °C). (b) Long columnar aragonite and hexagonal plate of vaterite (3.0×10^{-3} mol l^{-1}, 48.0 °C). (c) Columnar aragonite (1.5×10^{-3} mol l^{-1}, 75.5 °C). (d) Dendritic vaterite and long columnar aragonite (5.0×10^{-3} mol l^{-1}, 75.5 °C).

(figure 3). In order to discuss the conditions for the nucleation of metastable phases, let us assume a case where phase j is less stable than phase k, and compare both the steady state nucleation rates and induction period of two phases. Here we define two types of discriminates, $f_{(j/k)} = \ln[J_0(j)/J_0(k)]$ by using equation (2) and $g_{(j/k)} = \tau(j)/\tau(k)$ by using equation (3) as:

$$f_{(j/k)} = \frac{1}{2}\ln(\gamma_j/\gamma_k) - \frac{\Delta U_j - \Delta U_k}{k_B T} - \frac{16\pi}{3(k_B T)^3} \times \left[\frac{\gamma_j^3 \Omega_j^2}{(\ln AP - \ln K_j)^2} - \frac{\gamma_k^3 \Omega_k^2}{(\ln AP - \ln K_k)^2}\right], \quad (4)$$

$$g_{(j/k)} = \frac{\gamma_j}{\gamma_k}\frac{(\ln AP - \ln K_k)^2}{(\ln AP - \ln K_j)^2}\exp\left(\frac{\Delta U_j - \Delta U_k}{k_B T}\right), \quad (5)$$

where we assume that $C_i \nu_j \lambda_i \sim C_k \nu_k \lambda_k$ for simplicity.

When the phase j has a larger steady state nucleation rate ($f_{(j/k)} > 0$) and smaller induction period ($g_{(j/k)} < 1$) than the phase k, the phase j can nucleate first and appear as a primary phase in experiments. In the present paper, two types of diagrams are constructed to explain the nucleation processes of three polymorphs in the precipitation diagram (figure 3); one is the diagram where the phase with the largest steady state nucleation rate is plotted and the other the diagram where the phase with the lowest induction period is plotted in the $\ln AP$ versus T diagram (figure 5). Since the boundaries between primary phases are given by the conditions of $f_{(j/k)} = 0$ and $g_{(j/k)} = 1$, the regions around the boundaries can be considered to be co-precipitation zone. In the case where $f_{(j/k)} > 0$ and $g_{(j/k)} > 1$ or $f_{(j/k)} < 0$ and $g_{(j/k)} < 1$, the nucleation and following growth processes are not simple and the co-precipitation of two phases can also be expected.

Since the published values of γs (mJ m^{-2}) for the three polymorphs at 25 °C are γ_C = 7–280, γ_A = 150, and γ_V = 6.8–108, where C, A and V are calcite, aragonite and vaterite, respectively (Gómez-Morales *et al* 1996), we employ γ_C = 120 (Shönel and Mullin 1978, 1982), γ_A = 150 (Möller and Rajagopalan 1976), and γ_V = 40 (Gómez-Morales *et al* 1996) as the values at 25 °C in the calculation. When we assume constant values for the γs throughout the temperature range from 0 to 100 °C, and the same values of ΔUs for the three polymorphs, there is no area for the aragonite phase in a whole range of the diagrams (figures 5(a) and (b)), differing from the experimental diagram. This is simply understood from equations (4) to (5), because aragonite has a relatively large value of γ among the three polymorphs. The ΔUs, the activation energy for the attachment of molecules to the critical nuclei, must be similar among the three polymorphs. Even when ΔU of aragonite decreases relatively to those of other two polymorphs, the aragonite phase appears in a range with higher $\ln AP$ values than the vaterite range and almost parallel to the lines for equilibrium constants in the diagrams, differing from the appearance in the experimentally-determined diagram. Therefore, the precondition with the constant values of γs cannot explain the experimentally-determined diagram.

Another possibility where the value of γ_A decreases significantly with an increase of temperature is then considered

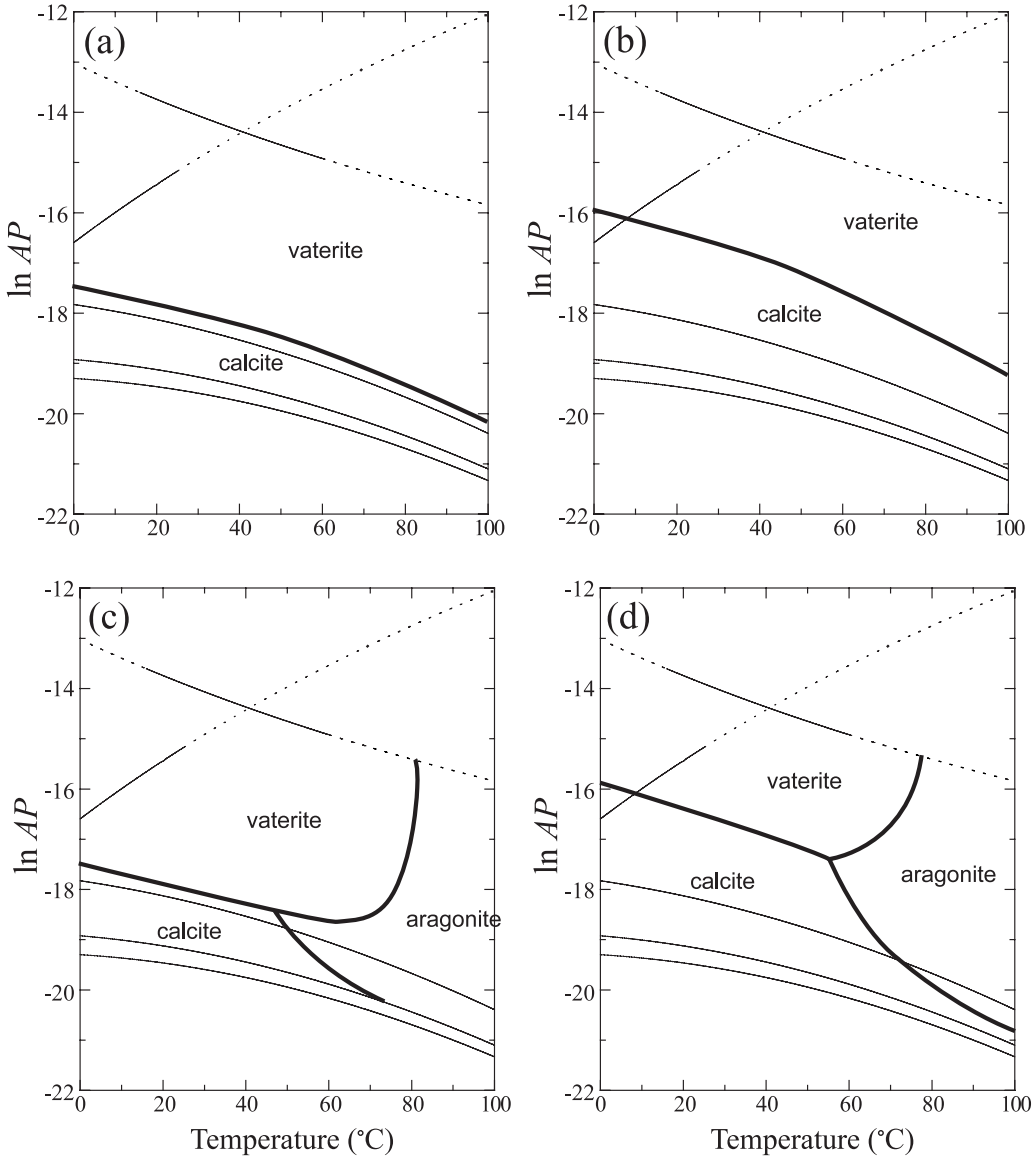

Figure 5. (a) and (c): precipitation diagrams on the appearance of phases with the largest steady state nucleation rate calculated by equation (4). (b) and (d): precipitation diagrams on the appearance of phases with the lowest induction period calculated by equation (5). Thick lines are boundaries between primary phases and thin lines are the equilibrium curves for polymorphs shown in figure 1. In the calculation, the activation energies: $\Delta U_C = \Delta U_A = \Delta U_V$ and the molar volumes: $\Omega_C = 6.13 \times 10^{-29}$, $\Omega_A = 5.64 \times 10^{-29}$, and $\Omega_V = 6.28 \times 10^{-29}$ m^3. Surface free energies for calcite and vaterite are kept constant at the values at 25 °C: $\gamma_C = 120$ and $\gamma_V = 40$ mJ m^{-2}. Surface free energy for aragonite is kept constant at $\gamma_A = 150$ mJ m^{-2} in (a) and (b), and changed as $\gamma_A = -1.8(T - 298) + \gamma_A^0$, where γ_A^0 is 150 mJ m^{-2} at 25 °C, in (c) and (d).

to explain the appearance of aragonite in the high temperature range. In the calculation, γ_C and γ_V are assumed to be constant and equal to the values at 25 °C and only γ_A is changed as $\gamma_A = -a(T - 298) + \gamma_A^0$, where a is constant and γ_A^0 is the value at 25 °C. The calculated diagrams were compared with the precipitation diagram (figure 3) by changing the value of a. The calculated diagrams with $a = 1.8$ (mJ m^{-2} K^{-1}) are shown in figures 5(c) and (d). Since the regions around the solid lines in the figures can be considered to be co-precipitation zones, four precipitation zones (calcite–vaterite co-precipitation zone, vaterite precipitation zone, vaterite–aragonite co-precipitation zone and aragonite precipitation zone) in the experimentally-determined diagram (figure 3) also appear in the regions with the similar values of ln AP and T in figures 5(c) and (d). This strong resemblance of the calculated to the experimentally-determined diagram suggests (1) the precipitation diagram can be well explained by nucleation theory, (2) the first-order importance of the surface free energies in the nucleation of the polymorphs and (3) the strong temperature dependency of the surface free energy of aragonite. The decrease of the relative values of γ_A with an increase in temperature suggests that aragonite has a stronger temperature dependency of surface entropy than the other two polymorphs.

The concepts obtained in the present study have important implications for investigating the impurity effect on the

formation of $CaCO_3$ (Kitano 1962a, 1962b). Addition of ions such as Mg^{2+}, which can form a solid solution with calcite, into a solution inhibits calcite formation and promotes aragonite formation. In contrast addition of ions such as Ba^{2+}, which can form a solid solution with aragonite, results in the opposite. These apparently paradoxical phenomena have been interpreted as the result of a decrease in supersaturation due to the addition of impurities (Davis *et al* 2000). The present study reveals the prime importance of surface free energies in the nucleation of the polymorphs, and that the aragonite precipitation range becomes larger as γ_A decreases. The present result implies there is also a strong impurity effect on the surface entropy of aragonite (or other polymorphs) due to absorption on the surface. Such an effect can also be expected in biological systems, such as aragonite formation in shellfish at ambient temperature and pressure.

Acknowledgments

We thank Dr S R Wallis for carefully reading the manuscript and his comments on it. Thanks are also due to two anonymous reviewers for critical readings of the manuscript. This study is partially supported by a Grant-in-Aid for Scientific Research from the Ministry of Education, Sports, Culture, Science, and Technology in Japan.

References

Aaronson H I and Lee J K 1999 The kinetic equations of solid → solid nucleation theory and comparisons with experimental observations *Lectures on the Theory of Phase Transformations* 2nd edn, ed H I Aaronson (Warrendale, PA: TMS) pp 165–225

Addadi L, Raz S and Weiner S 2003 Taking advantage of disorder: amorphous calcium carbonate and its roles in biomineralization *Adv. Mater.* **15** 959–70

Biscoff J L, Fitzpatrick J A and Rosenbauer R J 1993 The solubility and stabilization of ikaite $CaCO_3{\cdot}6H_2O$ from 0 to 25 °C: environmental and paleoclimatic implications for thinolite tufa *J. Geol.* **101** 21–33

Clarkson J R, Price T J and Adams D J 1992 Role of metastable phases in the spontaneous precipitation of calcium carbonate *J. Chem. Soc. Faraday Trans.* **88** 243–9

Davis K J, Dove P M and De Yoreo J 2000 The role of Mg^{2+} as an impurity in calcite growth *Science* **290** 1134–7

De Yoreo J and Vekilov P G 2003 Principles of crystal nucleation and growth *Biomineralization, Reviews in Mineralogy and Geochemistry* vol 54, ed P M Dove, J De Yoreo and S Weiner (Washington, DC: Mineralogical Society of America) pp 57–93

Falini G, Gazzano M and Ripamonti A 1994 Crystallization of calcium carbonate in presence of magnesium and polyelectrolytes *J. Cryst. Growth* **137** 577–84

Gómez-Morales J, Torrent-Burgués J and Rodríguez-Clemente R 1996 Nucleation of calcium carbonate at different initial pH conditions *J. Cryst. Growth* **169** 331–8

Johnston J, Merwin H E and Williamson E D 1916 The several forms of calcium carbonate *Am. J. Sci.* **4** 473–512

Kashchiev D 1969 Solution of the non-steady state problem in nucleation kinetics *Surf. Sci.* **14** 209–20

Kawano J, Shimobayashi N, Kitamura M, Shinoda K and Aikawa N 2002 Formation process of calcium carbonate from highly supersaturated solution *J. Cryst. Growth* **237–239** 419–23

Kitano Y 1962a The behaviour of various inorganic ions in the separation of calcium carbonate from a bicarbonate solution *Bull. Chem. Soc. Japan* **35** 1973–80

Kitano Y 1962b A study of the polymorphic formation of calcium carbonate in thermal springs with an emphasis on the effect of temperature *Bull. Chem. Soc. Japan* **35** 1980–5

Markov I V 1995 *Crystal Growth for Beginners: Fundamentals of Nucleation, Crystal Growth, and Epitaxy* (Singapore: World Scientific)

Möller P and Rajagopalan G 1976 Charges of excess free energies in the crystal growth process of calcite and aragonite due to the presence of Mg^{2+} ions in solution *Z. Phys. Chem. (NF)* **99** 187

Morse J W and Mackenzie F T 1990 *Geochemistry of Sedimentary Carbonates (Developments in Sedimentology)* (Amsterdam: Elsevier)

Nancollas G H, Sawada K and Schuttringer E 1983 Mineralization reactions involving calcium carbonates and phosphates *Biomineralization and Biological Metal Accumulation: Biological and Geological Perspectives* ed P Westbroek and E W de Jong (Berlin: Springer) pp 155–69

Ogino T, Suzuki T and Sawada K 1987 The formation and transformation mechanism of calcium carbonate in water *Geochim. Cosmochim. Acta* **51** 2757–67

Pina C M and Putnis A 2002 The kinetics of nucleation of solid solutions from aqueous solutions: a new model for calculation non-equilibrium distribution coefficients *Geochim. Cosmochim. Acta* **66** 185–92

Plummer L N and Busenberg E 1982 The solubilities of calcite, aragonite and vaterite in CO_2–H_2O solutions between 0° and 90°, and an evaluation of aqueous model for the system $CaCO_3$–CO_2–H_2O *Geochim. Cosmochim. Acta* **46** 1011–140

Shönel O and Mullin J W 1978 A method for the determination of precipitation induction periods *J. Cryst. Growth* **44** 377–82

Shönel O and Mullin J W 1982 Precipitation of calcium carbonate *J. Cryst. Growth* **60** 239–50

Toschev S 1973 Homogeneous nucleation *Crystal Growth: an Introduction* ed P Hartman (Amsterdam: North-Holland) pp 1–49

Weiner S and Dove P M 2003 An overview of biomineralization process and the problem of the vital effect *Biomineralization, Reviews in Mineralogy and Geochemistry* vol 54, ed P M Dove, J De Yoreo and S Weiner (Washington, DC: Mineralogical Society of America) pp 1–29